Figure 1.42. System block diagram.

■ 1.5 Sampling

■ 1.5.1 Motivation

As we have covered the basic theoretical foundations and start considering several practical issues, it is useful to briefly summarize what we have accomplished so far and to motivate what lies ahead.

We started by considering some examples of signal processing algorithms in action, and saw that all those examples fit into one basic picture (Fig. 1.42). We have talked about a few very basic notions, which the whole field of signal processing is based on, such as the notions of signals and systems. We concentrated on linear time-invariant systems and saw that in order to analyze such systems, it was important to study representations of signals in orthogonal bases:

$$s(n) = \sum_k a_k g_k(n).$$

For example,

- when we represented our input signal as the sum of shifted and scaled impulses, we obtained the interpretation of an LTI system as the convolution of its impulse response with the input.

- when we represented our input signal as the sum of complex exponentials, we got an equally important interpretation of an LTI system–namely, that it modifies different frequency components independently of each other, by multiplying each component by a complex number. We called these frequency-dependent complex numbers the frequency response and saw that it was the discrete-time Fourier transform of the impulse response. We moreover studied the FFT which a fast algorithm for computing spectral representations of signals–specifically, the DFT.

Because of these properties of LTI systems, it is very important to be able to think of signals both in time domain and in frequency domain.

The background material that we covered allows us to begin considering several important practical matters. One example which will be considered in the lab portion of this course, is filter design, where the goal may be to attenuate certain frequencies in a signal and enhance other frequencies. Every time you adjust the bass or treble on your audio equipment, you are modifying a digital filter. Every time you click "enhance" in an image editing program, you are applying a digital filter to the image.

Another practical issue that we will start studying shortly is sampling. You may have noticed that most real-world signals are continuous-time or continuous-space. When you go to a concert, the music you hear is a continuous-time signal. How can you reliably store it as discrete samples on a compact disc? Similarly, the world you see around you is continuous. How can we store digital images on a computer and make them look realistic and distortion-free? Sampling theory will provide partial answers to these questions.

■ 1.5.2 Ideal Sampling

In the following, we denote the sampling period by T_s and the sampling frequency by $f_s = \frac{1}{T_s}$. We begin by summarizing some facts about continuous-time signals.

CTFT The forward and inverse continuous-time Fourier transform (CTFT) formulas are:

$$\begin{aligned} X(f) &= \int_{-\infty}^{\infty} x(t)e^{-j2\pi ft}dt, \\ x(t) &= \int_{-\infty}^{\infty} X(f)e^{j2\pi ft}df. \end{aligned}$$

It is possible to extend the definition of the CTFT to generalized functions called *tempered distributions*. One example of a tempered distribution is the continuous-time impulse $\delta(t)$. In this framework, it can be shown that the Poisson formula holds:

$$s(t) = \sum_{n=-\infty}^{\infty} \delta(t - nT_s) \quad \longrightarrow \quad S(f) = \frac{1}{T_s} \sum_{n=-\infty}^{\infty} \delta\left(f - \frac{n}{T_s}\right),$$

i.e., that the CTFT of a periodic impulse train is another periodic impulse train, as shown in Fig. 1.43.

Convolution with $\delta_{t_0}(t) = \delta(t - t_0)$ is simply a translation by t_0:

$$x * \delta_{t_0}(t) = \int_{-\infty}^{\infty} \delta(\tau - t_0)x(t - \tau)d\tau = x(t - t_0).$$

We represent the ideal sampling process as a multiplication of a signal by a periodic train of continuous-time impulses, as shown in Fig. 1.44. Referring to this system, we have:

$$\begin{aligned} x_s(t) = x_c(t)s(t) \quad \longrightarrow \quad X_s(f) &= X_c * S(f) \\ &= \frac{1}{T_s} \sum_{n=-\infty}^{\infty} X_c\left(f - \frac{n}{T_s}\right). \end{aligned} \tag{1.36}$$

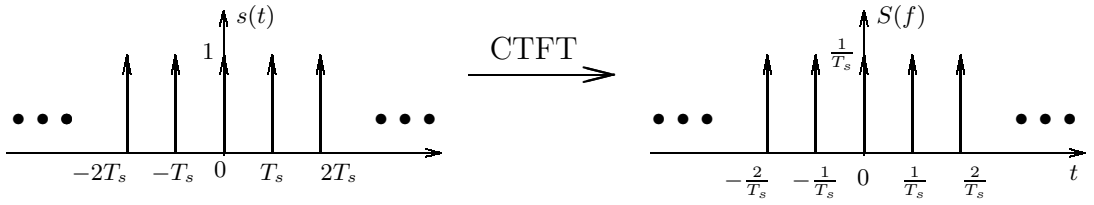

Figure 1.43. CTFT of a periodic impulse train.

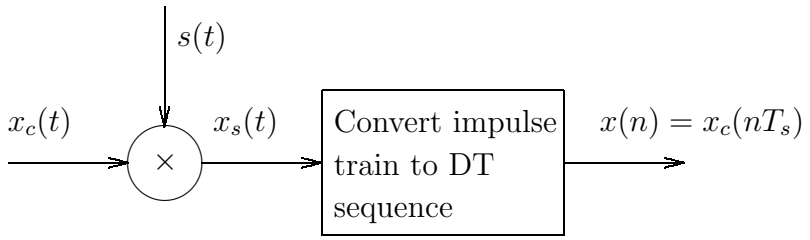

Figure 1.44. Block diagram of an ideal sampler.

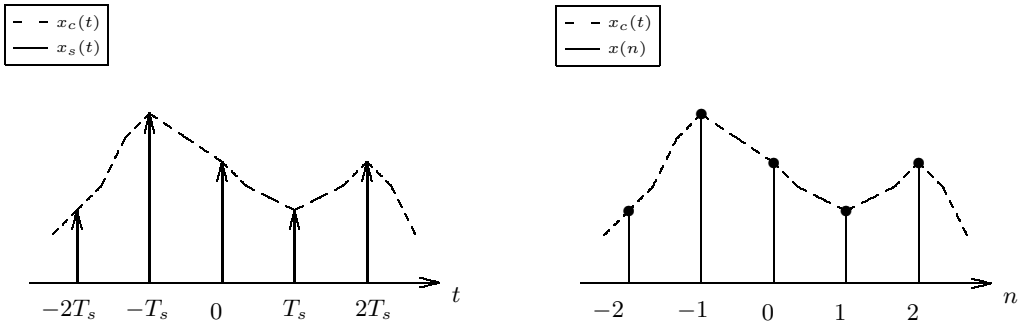

(a) The signals $x_c(t)$ and $x_s(t)$.

(b) The signals $x_c(t)$ and $x(n)$.

Figure 1.45. An example of $x_c(t)$ and the resulting $x_s(t)$ and $x(n)$ for Fig. 1.44.

To analyze what happens in the frequency domain, we need to relate the DTFT of $x(n)$ to the CTFT's of $x_s(t)$ and $x_c(t)$. We do this by using a different method to calculate the CTFT of $x_s(t)$.

$$\begin{aligned} x_s(t) &= \sum_{n=-\infty}^{\infty} x_c(nT_s)\delta(t-nT_s) \\ X_s(f) &= \sum_{n=-\infty}^{\infty} x_c(nT_s)\mathrm{CTFT}\{\delta(t-nT_s)\} \\ &= \sum_{n=-\infty}^{\infty} x_c(nT_s)\left\{\int_{-\infty}^{\infty}\delta(t-nT_s)e^{-j2\pi ft}dt\right\} \\ &= \sum_{n=-\infty}^{\infty} x(n)e^{-j2\pi fT_s n} \\ &= X(e^{j\omega})|_{\omega=2\pi fT_s}. \end{aligned}$$

Therefore,

$$\begin{aligned} \underbrace{X_s(f)}_{\texttt{CTFT of } x_s(t)} &= \underbrace{X(e^{j2\pi fT_s})}_{\texttt{DTFT of } x(n)} \\ X(e^{j\omega}) &= X_s\left(\frac{\omega}{2\pi T_s}\right). \end{aligned}$$

From this derivation, we see that in order to get $X\left(e^{j\omega}\right)$ from $X_s(f)$, we just need to rescale the frequency axis by replacing f_s with 2π, $\frac{f_s}{2}$ with π etc.

We can now use Eq. (1.36) to express the spectrum of the DT sampled signal in terms of the spectrum of the original CT signal $x_c(t)$:

$$X(e^{j\omega}) = X_s\left(\frac{\omega}{2\pi T_s}\right) = \frac{1}{T_s}\sum_{n=-\infty}^{\infty} X_c\left(\frac{\omega}{2\pi T_s} - \frac{n}{T_s}\right).$$

The major point of concern here is how accurately these discrete samples represent the original CT signal. We will try to answer this question by looking at the spectra and determining whether the original spectrum $X_c(f)$ can be recovered by low-pass filtering $X(e^{j\omega})$.

Example 1.28. *Sampling and reconstruction.*

Consider a signal with the spectrum of Fig. 1.46. Under what circumstances can we reconstruct this signal from its samples by ideal low-pass filtering?

Case 1. $\frac{f_s}{2} > a$.

In this case, the spectrum of the continuous-time sampled signal $x_s(t)$ is given in Fig. 1.47. The original spectrum of Fig. 1.46 can clearly be recovered by filtering

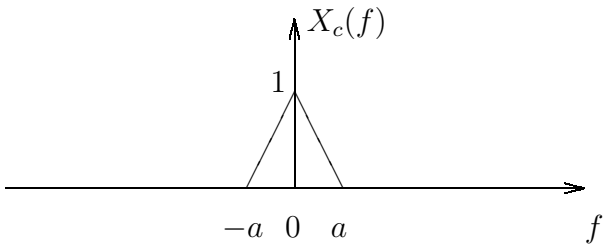

Figure 1.46. Spectrum of the continuous-time signal $x_c(t)$ of Example 1.28.

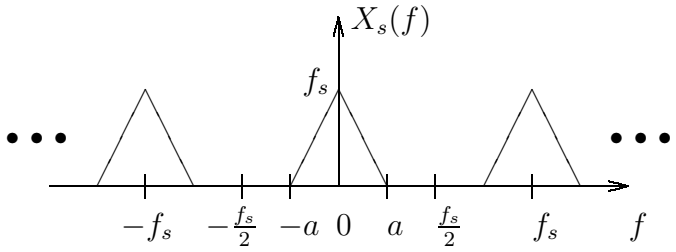

Figure 1.47. Spectrum of the sampled continuous-time signal $x_s(t)$ from Example 1.28 when the sampling rate is greater than $2a$.

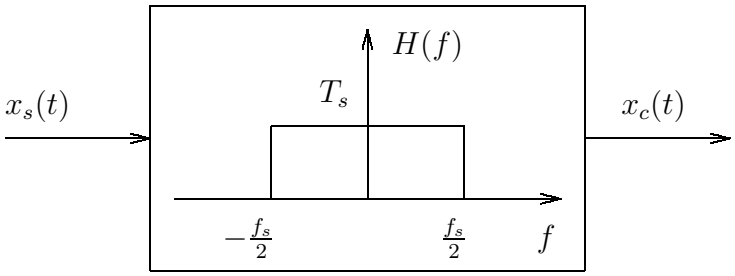

Figure 1.48. Reconstruction of $x_c(t)$ from $x_s(t)$. If the sampling rate is higher than $2a$, perfect reconstruction with an ideal low-pass filter is possible.

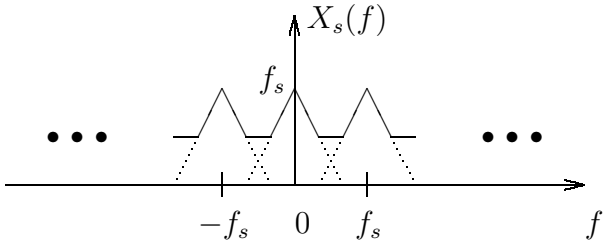

Figure 1.49. Spectrum of the sampled continuous-time signal $x_s(t)$ from Example 1.28 when the sampling rate is less than $2a$.

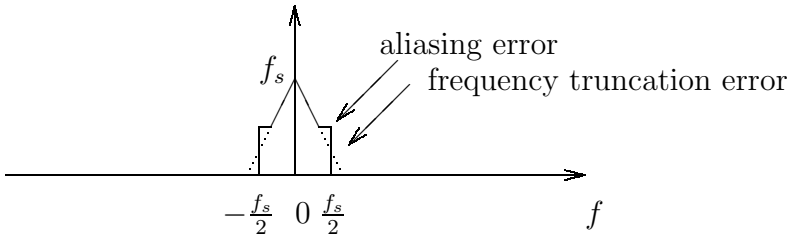

Figure 1.50. Spectrum of recovered aliased signal of Example 1.28.

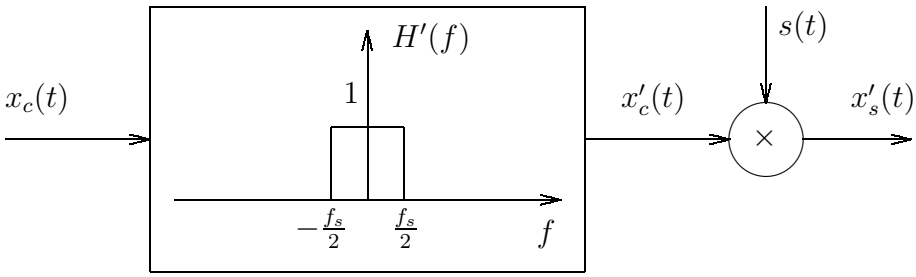

Figure 1.51. Illustration to Example 1.28, Case 2: prefiltering before sampling.

$X_s(f)$ with an ideal low-pass filter whose cutoff frequency is $f_s/2$. This is shown in Fig. 1.48. Thus, perfect reconstruction with an ideal low-pass filter is possible if the sampling frequency is larger than twice the highest frequency of the signal.

Case 2. *$\frac{f_s}{2} \leq a$. Referring to Fig. 1.49, we see that it is impossible to recover x_c with a low-pass filter without distortion. The distortion occurs because the spectra of neighboring copies interfere with the original spectrum. When we filter $X_s(f)$ with $H(f)$, we recover the distorted signal whose spectrum is shown in Fig. 1.50.*

One possible way of avoiding this distortion is, as we have seen in Case 1, to sample at a higher rate. However, if we cannot sample at a higher rate, there is still something that we can do in order to improve the quality of the reconstruction. Specifically, we can prefilter the continuous-time signal before sampling, to ensure that the highest frequency of the signal to be sampled is not larger than $\frac{f_s}{2}$ (Fig. 1.51). Let $x'_c(t)$ be the result of prefiltering $x_c(t)$ with the ideal low-pass filter $H'(f)$ depicted in Fig. 1.51. Let $x'_s(t)$ be the corresponding continuous-time sampled signal. If we now try to recover $x_c(t)$ from $x'_s(t)$ with our ideal low-pass filter $H(f)$, we get back $x'_c(t)$. Its spectrum, depicted in Fig. 1.52(a), is closer to the original spectrum than our previous result of Fig. 1.50. The frequencies in the range $[f_s - a, \frac{f_s}{2}]$ are now recovered–in other words, the aliasing error is removed. (The frequency truncation error is, however, still present.)

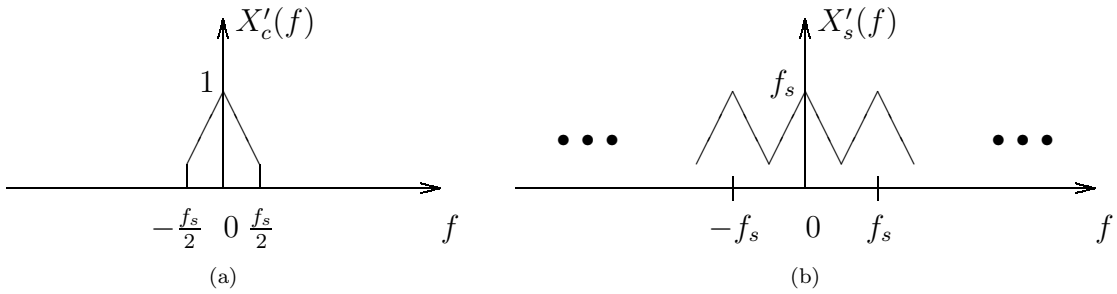

Figure 1.52. Effects of prefiltering, sampling, and reconstruction on the spectrum of the signal of Example 1.28, Case 2. (a) The spectrum which results from prefiltering with an ideal low-pass filter; (b) the spectrum of the sampled prefiltered signal. The prefiltered signal can be reconstructed from the samples by ideal low-pass filtering.

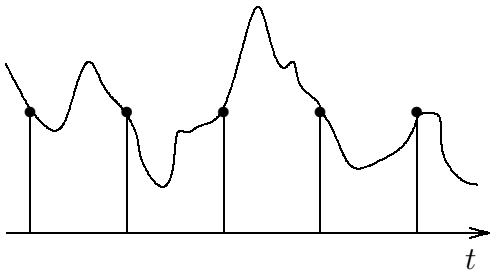

Figure 1.53. If sampling rate is lower than the Nyquist rate, some information about the continuous-time signal will be lost in the sampled signal.

■ 1.5.3 Nyquist Sampling Theorem

Let $x_c(t)$ be a band-limited signal with

$$X_c(f) = 0, \text{ for } |f| > a.$$

The parameter a is called the Nyquist frequency, and $2a$ is called the Nyquist rate. If $x_c(t)$ is sampled at the rate of f_s samples per second which is larger than the Nyquist rate,

$$f_s > 2a,$$

then $x_c(t)$ can be recovered from its samples,

$$x(n) = x_c(nT), \ n = 0, \pm 1, \pm 2, \ldots,$$

by ideal low-pass filtering. If there is no restriction on the bandwidth of the signal, unique reconstruction from samples is impossible. This is illustrated in Fig. 1.53 where the discrete samples form a constant signal whereas the continuous-time signal is allowed to change rapidly between the samples.

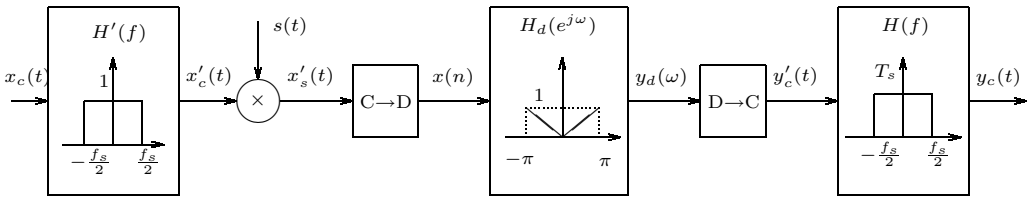

Figure 1.54. A system for sampling, DT processing, and reconstruction (Example 1.29).

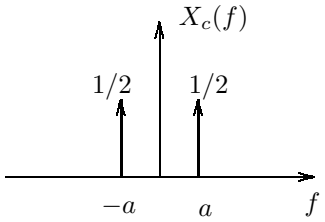

Figure 1.55. Input spectrum $X_c(f)$ to the system of Example 1.29.

Example 1.29. *DT processing of CT signals.*
Suppose we wanted to convert an old analog recording to digital format, store it on a compact disc (CD) and then play it back on a CD player. Fig. 1.54 illustrates, in a very idealized manner, the steps we would take. Note that before storing the signal on a CD, we might want to do some signal processing, for example, in order to enhance the quality of the audio signal. This step is represented by H_d. Once we have our CD, we would like to play it on our audio equipment–i.e. we would like to convert the DT signal on the CD to a CT music signal.

While this diagram is just a simple example, its structure is quite similar to the structure of real systems. In Example 1.28, we considered every component of this diagram except for the middle portion (DT processing). Let us consider how this system will process the input signal whose Fourier transform $X_c(f)$ is depicted in Fig. 1.55.

First, we use the inverse CTFT formula to calculate the signal $x_c(t)$:

$$\begin{aligned} x_c(t) &= \int_{-\infty}^{\infty} X_c(f) e^{j2\pi ft} df \\ &= \frac{1}{2}\int_{-\infty}^{\infty} \delta(f-a) e^{j2\pi ft} df + \frac{1}{2}\int_{-\infty}^{\infty} \delta(f+a) e^{j2\pi ft} df \\ &= \frac{1}{2} e^{j2\pi at} + \frac{1}{2} e^{-j2\pi at} \\ &= \cos(2\pi at). \end{aligned}$$

Now we consider the same two cases as in Example 1.28.

Case 1 $f_s > 2a$.

1. $X_c'(f) = X_c(f)H'(f)$

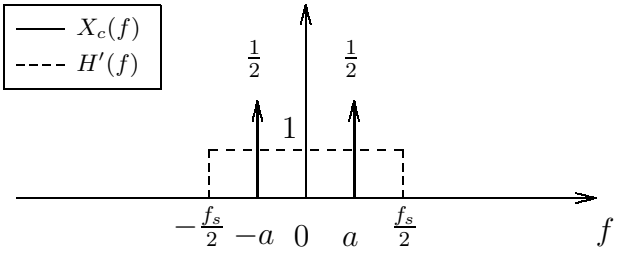

2. $X_s'(f) = X_c'(f) * S(f)$

$$= X_c'(f) * \tfrac{1}{T_s} \sum_{n=-\infty}^{\infty} \delta\left(f - \tfrac{n}{T_s}\right)$$

$$= \tfrac{1}{T_s} \sum_{n=-\infty}^{\infty} X_c'\left(f - \tfrac{n}{T_s}\right)$$

(recall that $f_s = \frac{1}{T_s}$.)

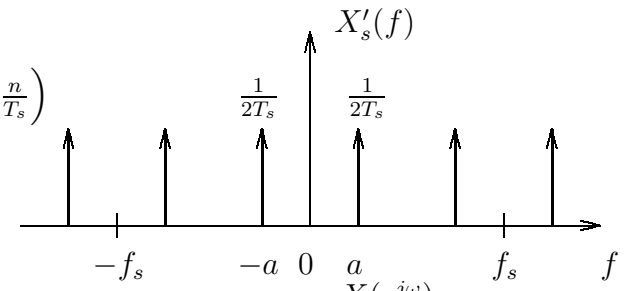

3. $X(e^{j\omega}) = X_s'\left(\frac{\omega}{2\pi T_s}\right)$

Rescale the frequency axis.

Also, adjust the areas of the δ's:

recall that $\delta(a\omega) = \frac{1}{|a|}\delta(\omega)$,

and so

$\frac{1}{2T_s}\delta\left(\frac{\omega}{2\pi T_s}\right) = \frac{2\pi T_s}{2T_s}\delta(\omega) = \pi\delta(\omega)$

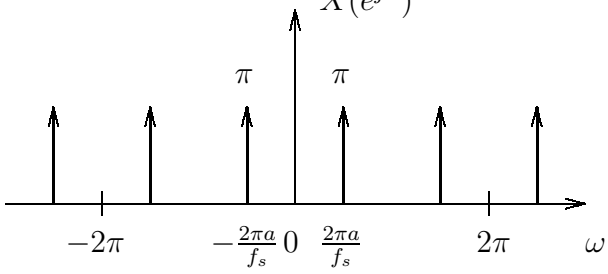

4. $Y_d(e^{j\omega}) = X(e^{j\omega})H_d(e^{j\omega})$,

where

$$H_d(e^{j\omega}) = \begin{cases} \frac{\omega}{\pi}, & 0 \le \omega \le \pi \\ -\frac{\omega}{\pi}, & -\pi \le \omega \le 0 \end{cases}$$

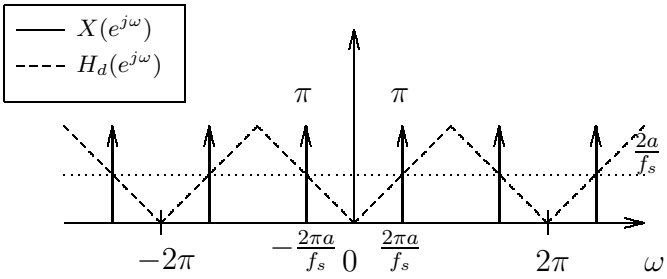

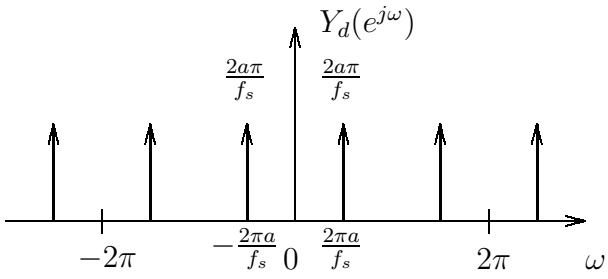

5. To get $Y_c'(f)$, re-label the frequency axis back and rescale the impulses.

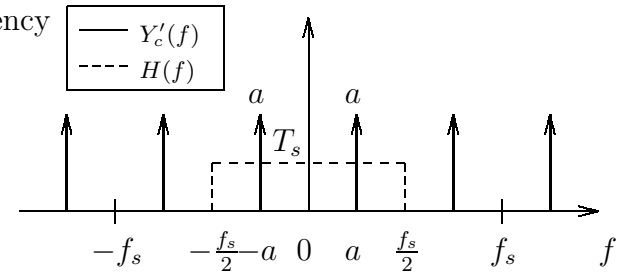

6. $Y_c(f) = Y_c'(f)H(f) =$

$$= \begin{cases} T_s Y_c'(f) & |f| \le \frac{f_s}{2} \\ 0 & |f| > \frac{f_s}{2} \end{cases}$$

$$= T_s a\{\delta(f-a) + \delta(f+a)\}$$

$$\Rightarrow y(t) = 2aT_s \cos 2\pi a t$$

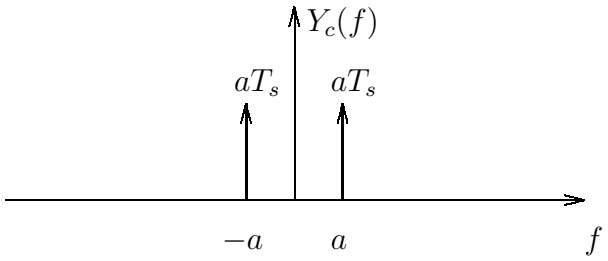

Therefore, the overall effect of the system on this particular input signal is equivalent to multiplication by $2aT_s$.

Case 2. $f_s < 2a$.

In this case, the output will be zero because the whole input signal will be filtered out by the first low-pass filter $H'(f)$.

Let us now look closer at the reconstruction of an ideally sampled signal. First, we assume that there is no prefiltering.

Assume that after sampling a continuous-time signal $x_c(t)$, we get the samples $x_s(t)$ as in Fig. 1.57(a). What happens when $x_s(t)$ goes through the low-pass filter as in Fig. 1.56? Note that the comb function $s(t)$ and the low-pass filter $H(f)$ are as previously defined in Example 1.29, and thus we have:

$$x_s(t) = \sum_n x_c(nT_s)\delta(t - nT_s)$$

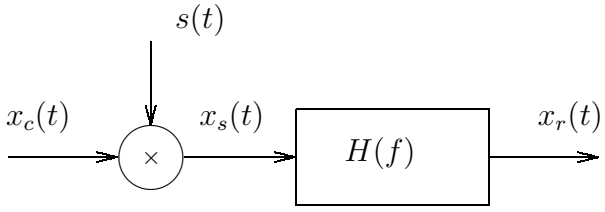

Figure 1.56. Signal reconstruction system.

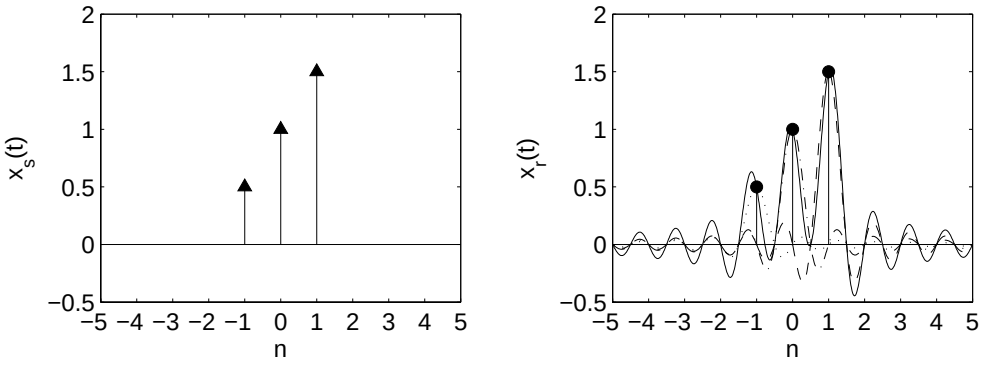

(a) $x_s(t)$ of the system in Fig. 1.56.

(b) The reconstructed signal $x_r(t)$.

Figure 1.57. Interpolation with sincs.

The reconstructed spectrum is

$$X_r(f) = X_s(f)H(f),$$

therefore,

$$\begin{aligned} x_r(t) &= x_s(t) * h(t) \\ &= x_s(t) * \mathrm{sinc}(f_s t) \\ &= \left\{ \sum_n x_c(nT_s)\delta(t - nT_s) \right\} * \mathrm{sinc}(f_s t) \\ &= \sum_n x_c(nT_s)\mathrm{sinc}(f_s(t - nT_s)), \end{aligned} \tag{1.37}$$

where we used the inverse CTFT formula to obtain $h(t)$:

$$\begin{aligned} h(t) &= \int_{-\infty}^{\infty} H(f)e^{j2\pi ft}df \\ &= \frac{T_s}{j2\pi t} e^{j2\pi ft} \Big|_{f=-\frac{f_s}{2}}^{f=\frac{f_s}{2}} \\ &= \mathrm{sinc}(f_s t). \end{aligned}$$

From Eq. (1.37), it is seen that, in the time domain, reconstruction by low-pass filtering is equivalent to interpolating the DT signals with sinc functions. The sinc functions are scaled and added up together to form the reconstructed signal (Fig. 1.57). Again, we have a representation of the form:

$$x_r(t) = \sum_k a_k g_k(t),$$

where now g_k's are sinc functions.

The original CT signal $x_c(t)$ may contain frequencies above $\frac{f_s}{2}$. However, prefiltering $x_c(t)$ with an LPF to avoid aliasing is the orthogonal projection of the signal onto the space of all bandlimited signals with highest frequency $\frac{f_s}{2}$, as shown in Fig. 1.58. This results in a reconstruction which is the closest to $x_c(t)$ among all possible signals in this space (Fig. 1.58).

It turns out that $\{\text{sinc}(f_s(t - nT_s))\}_{n=-\infty}^{\infty}$ is an orthogonal basis for this space.

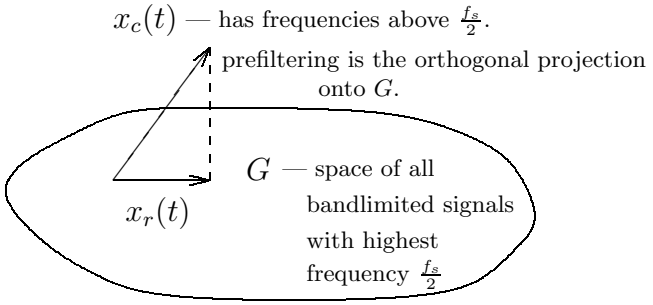

Figure 1.58. Prefiltering with an LPF to avoid aliasing is the orthogonal projection of the original signal on to the space, G of all bandlimited signals with highest frequency $\frac{f_s}{2}$.

Why is this interpretation important? The space of all bandlimited signals is good for approximating smooth signals whose energy is concentrated at low frequencies. It is well adapted to sound recordings, which are well approximated by lower frequency harmonics.

For discontinuous signals, such as images, a low-frequency restriction produces the *Gibbs oscillations*. If you try to approximate a square pulse (Fig. 1.59(a)) with low-frequency components, you will get a reconstruction which looks like Fig. 1.59(b).

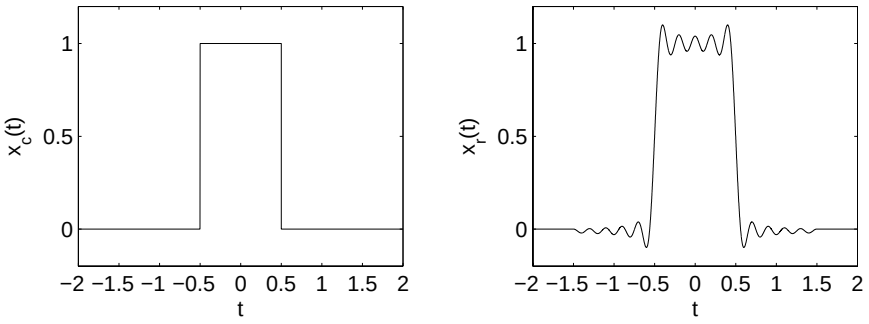

(a) A square pulse.

(b) Reconstruction with Gibbs oscillations.

Figure 1.59. The effects of Gibbs oscillations.

The visual quality of images is degraded by these oscillations, so it is not a good

idea to sample images in the same way sound signals are sampled. For the sampling and reconstruction of images, it may be better to pick a basis which is different from the sinc basis, and to project onto a different subspace. However, the basic vector-space paradigm will remain the same.

This is yet another illustration of the importance of linear algebra in signal processing. It is very important to get used to thinking about signals as vectors. This allows one to get a broader view–namely, that much of what we have done in this course is decomposing signals into different bases and working with projections of signals onto the bases vectors. We have seen that this is the basic idea behind convolution, frequency analysis and also, sampling.

We next consider several deviations from the ideal sampling model.

■ 1.5.4 Effects of Zero-Order Hold Sampling

It is impossible to produce ideal impulses of infinite energy and zero duration. Real systems try to get around this by using the sample-and-hold scheme, where the value of a sample is held until the value of the next sample is available. So instead of an impulse train, the result of this sampling operation is a staircase function x_{ZOH} (Fig. 1.60). This function can be represented as the convolution of the ideally sampled signal $x_s(t)$ and a square pulse $q(t)$, as shown in Fig. 1.60.

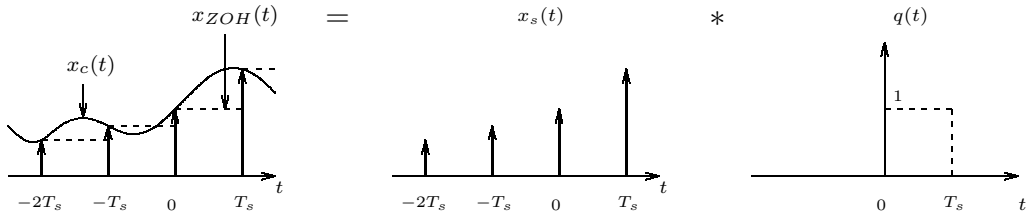

Figure 1.60. The staircase function which results from the sample-and-hold is equal to the ideally sampled signal convolved with a square pulse.

Therefore,

$$\begin{aligned} X_{ZOH}(f) &= X_s(f) \cdot CTFT\{q(t)\} \\ &= X_s(f) \int_{-\infty}^{\infty} q(t) e^{-j2\pi ft} dt \\ &= X_s(f) \int_{0}^{T_s} e^{-j2\pi ft} dt \\ &= X_s(f) \frac{1}{\pi f} \left[-\frac{1}{2j} e^{-j2\pi ft} \Big|_0^{T_s} \right] \\ &= X_s(f) \frac{1}{\pi f} \left[\frac{1}{2j} \left(1 - e^{-j2\pi fT_s} \right) \right] \end{aligned}$$

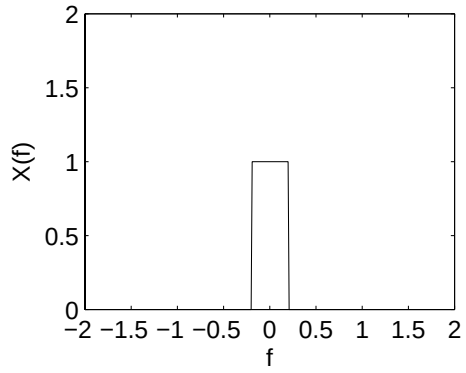

(a) The original spectrum.

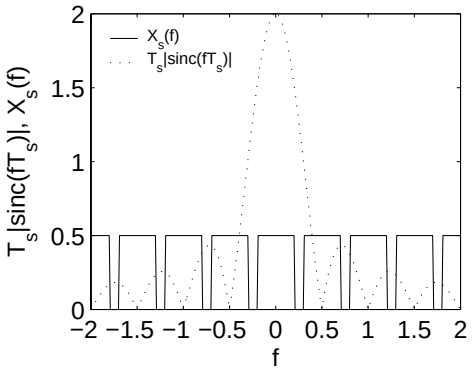

(b) Sample-and-hold for $f_s = 0.5$.

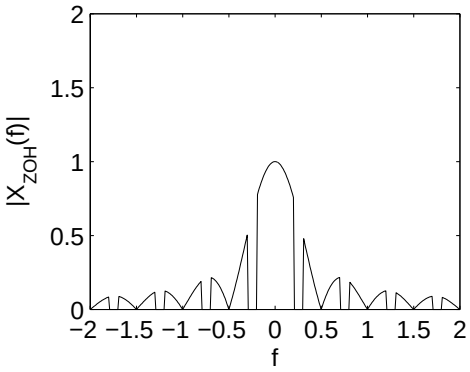

(c) $|X_{ZOH}(f)|$ for $f_s = 0.5$.

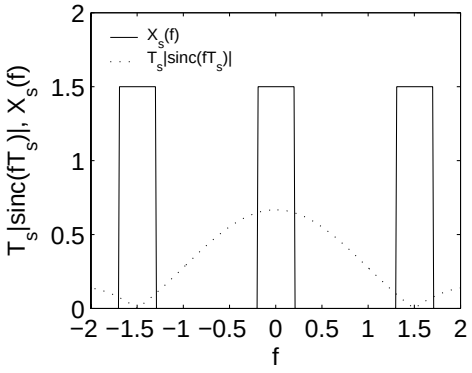

(d) Sample-and-hold for $f_s = 1.5$.

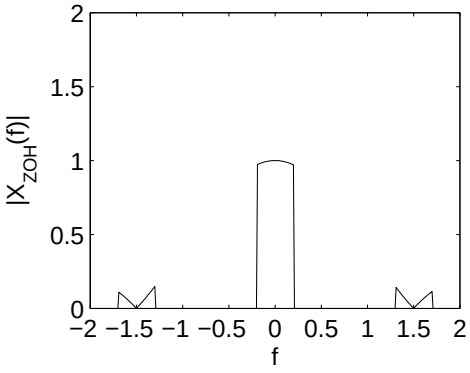

(e) $|X_{ZOH}(f)|$ for $f_s = 1.5$.

Figure 1.61. An illustration of the sample-and-hold scheme. (a) The original spectrum. (b) The ideally sampled spectrum $X_s(f)$ and the magnitude of the spectrum of the square pulse $q(t)$ for $f_s = 0.5$. (c) The magnitude of the spectrum of the signal obtained with sample-and-hold, which is the product of the two spectra in (b). (d,e) The same experiment with sampling rate $f_s = 1.5$.

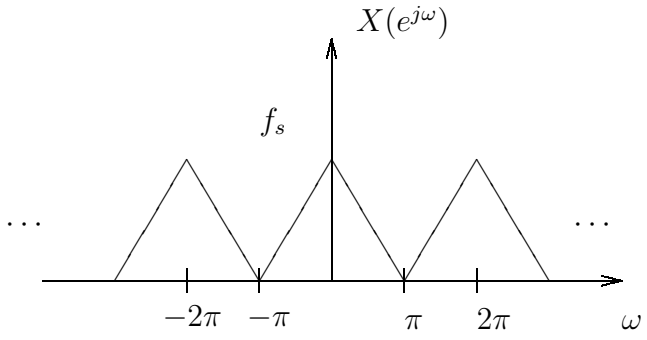

Figure 1.62. Sampling at Nyquist rate.

$$\begin{aligned} &= X_s(f)\frac{1}{\pi f}e^{-j\pi fT_s}\left[\frac{1}{2j}\left(e^{j\pi fT_s}-e^{-j\pi fT_s}\right)\right] \\ &= X_s(f)T_s e^{-j\pi fT_s}\frac{\sin(\pi fT_s)}{\pi fT_s} \\ &= X_s(f)T_s e^{-j\pi fT_s}\mathrm{sinc}(fT_s) \end{aligned}$$

Hence, $|X_{ZOH}(f)| = T_s|X_s(f)| \cdot |\mathrm{sinc}(fT_s)|$, i.e., $X_{ZOH}(f)$ is a distorted version of $X_s(f)$, as exemplified by Fig. 1.61(b,c). One possible method of reducing the distortion is to oversample, i.e., to increase the sampling rate beyond the Nyquist rate. As shown in Fig. 1.61(d,e), this both spreads the aliases farther apart, and makes the center alias less distorted.

■ 1.5.5 Discrete-Time Interpolation: Increasing the Sampling Rate

Another important deviation from the ideal scenario is that it is impossible to build an ideal analog low-pass filter — that is, a filter which would be exactly a non-zero constant for some range of frequencies and exactly zero everywhere else. Moreover, it is very difficult and expensive to build even a good approximation to such a filter. However, it is much easier to build a good digital filter that performs this function. What are the implications? Suppose we sampled at the Nyquist rate, barely avoiding aliasing (Fig. 1.62). Just converting to CT and reconstructing will not work, as we would need an ideal filter. Instead, we could partially solve this problem in DT by *interpolating*, as shown in Fig. 1.63.

Interpolation consists of two steps: upsampling and low-pass filtering.

Step 1. Upsampling by a factor of L is inserting $L-1$ zeros after each sample:

$$\begin{cases} x_u(Ln) &= x(n) \\ x_u(Ln+1) &= x_n(Ln+2) = \cdots = x_u(Ln+L-1) = 0 \end{cases}$$

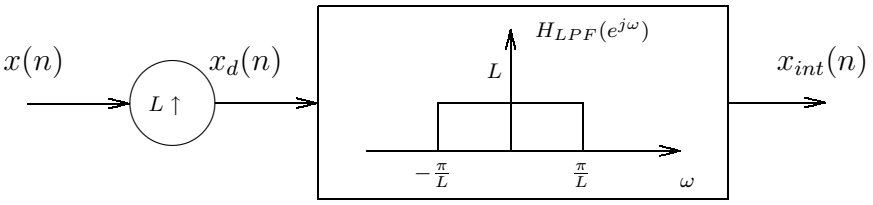

Figure 1.63. System diagram of an interpolation scheme.

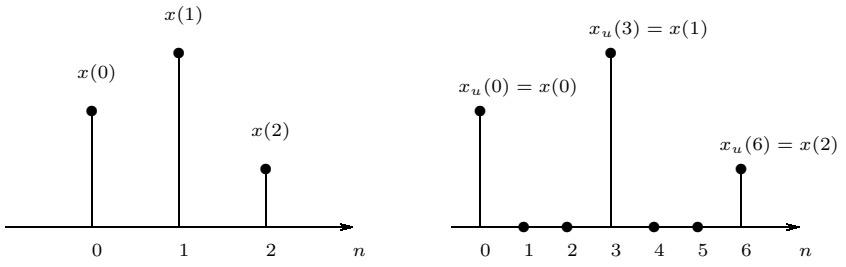

(a) A DT signal. (b) The result of upsampling with $L = 3$.

Figure 1.64. Upsampling a signal.

An example with $L = 3$ is shown in Fig. 1.64. Therefore,

$$\begin{aligned} X_u(e^{j\omega}) &= \sum_k x_u(k)e^{-j\omega k} \\ &= \sum_n x_u(Ln)e^{-j\omega Ln}, \text{since } x_u(k) \neq 0 \text{ only if } k \text{ is an integer multiple of } L \\ &= \sum_n x(n)e^{-j(\omega L)n} \\ &= X(e^{j\omega L}). \end{aligned}$$

Step 2. Low-pass filter the interpolated signal.

How is the signal reconstructed? We begin from Fig. 1.65(c),

$$x_{int(n)} = x_u * h(n) \tag{1.38}$$

where $h(n)$ is the impulse response of the low-pass filter–i.e., it is the inverse DTFT of H_{LPF} of Fig. 1.65(b):

$$\begin{aligned} h(n) &= \frac{1}{2\pi}\int_{-\pi}^{\pi} H_{LPF}\left(e^{j\omega}\right)e^{j\omega n}d\omega \\ &= \frac{1}{2\pi}\int_{-\frac{\pi}{L}}^{\frac{\pi}{L}} Le^{j\omega n}d\omega \end{aligned}$$

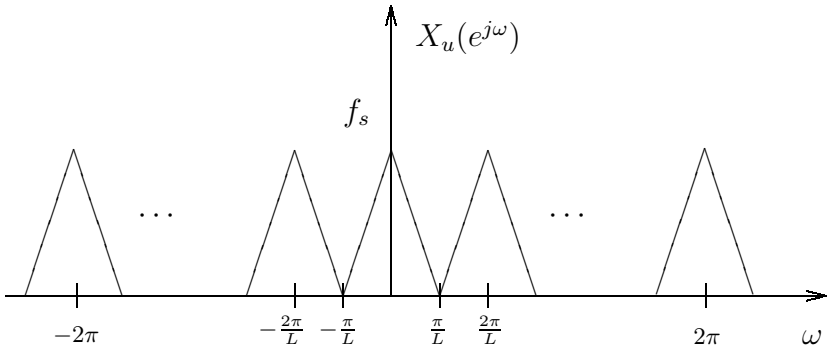

(a) Input signal spectrum before interpolation.

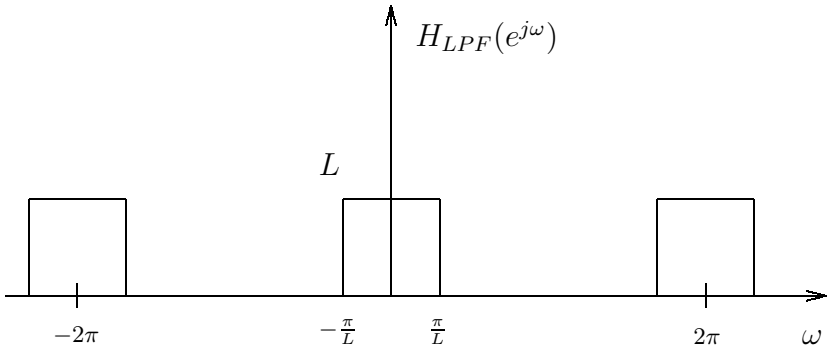

(b) Spectral characteristic of the low-pass filter.

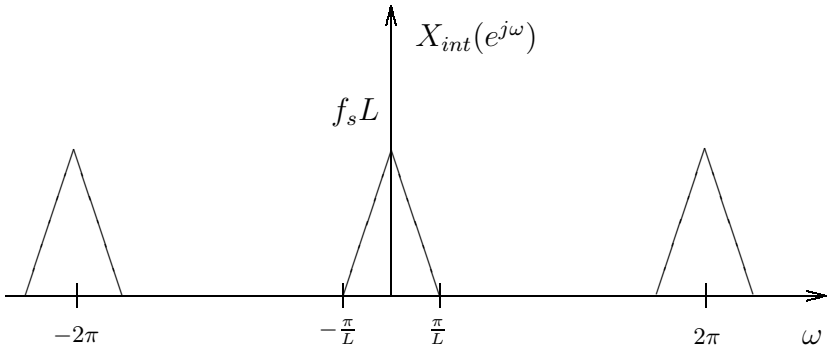

(c) Input signal spectrum after interpolation.

Figure 1.65. The effects of interpolation on the spectrum of input signal x.

$$\begin{aligned} &= \frac{L}{2\pi jn}\ e^{j\omega n}\Big|_{\omega=-\frac{\pi}{L}}^{\omega=\frac{\pi}{L}} \\ &= \frac{L}{\pi n}\sin\frac{\pi n}{L} \\ &= \operatorname{sinc}\left(\frac{n}{L}\right) \end{aligned} \tag{1.39}$$

Putting Eq. (1.39) into Eq. (1.38), we have the following:

$$\begin{aligned} x_{int(n)} &= \sum_k x_u(k)\text{sinc}\left(\frac{n-k}{L}\right) \\ &= \sum_m x_u(mL)\text{sinc}\left(\frac{n-mL}{L}\right) \\ &= \sum_m x(m)\text{sinc}\left(\frac{n-mL}{L}\right) \end{aligned} \tag{1.40}$$

Now we can get away with a poor analog LPF and still reconstruct the original signal very well, because the signal spectrum replicas are further apart (Fig. 1.65(c)).

Note that Eq. (1.40) has a form that is similar to the CT reconstruction formula, Eq. (1.37),

$$x_r(t) = \sum_n x(n)\text{sinc}\left(\frac{t-nT_s}{T_s}\right).$$

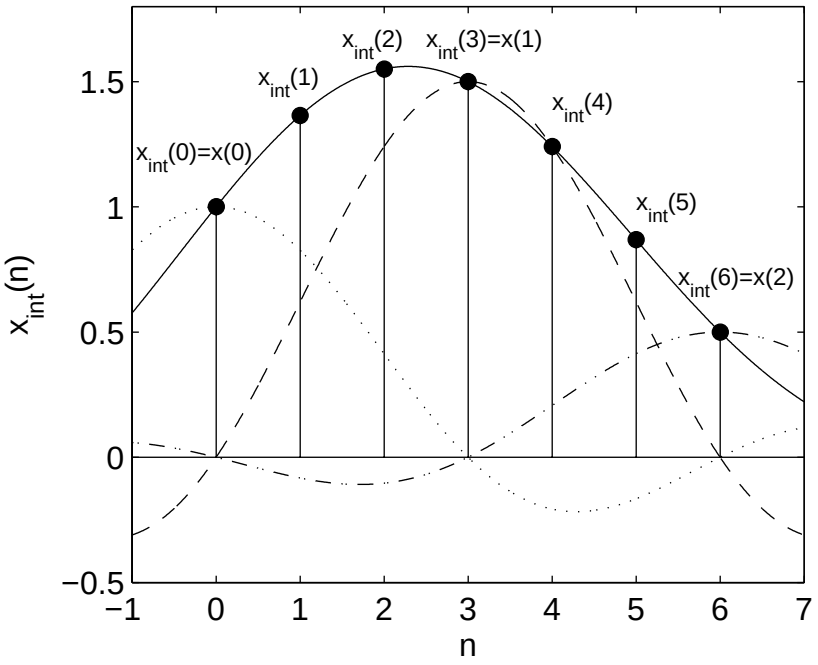

Figure 1.66. Low-pass filtering the upsampled signal interpolates the reconstructed data points via sinc functions.

As in the continuous-time case, the reconstruction is produced by a series of sinc functions. It is good for slowly varying signals but not good for signals with sharp transitions because of Gibbs oscillations.

■ 1.5.6 Decimation: Decreasing Sampling Rate

There are situations where we may have to decrease the sampling rate, e.g. due to the lack of processing speed or the lack of available memory.

Downsampling by a factor of D is taking every D-th sample from a DT signal:

$$x_d(n) = x(Dn). \tag{1.41}$$

It is illustrated in Fig. 1.67.

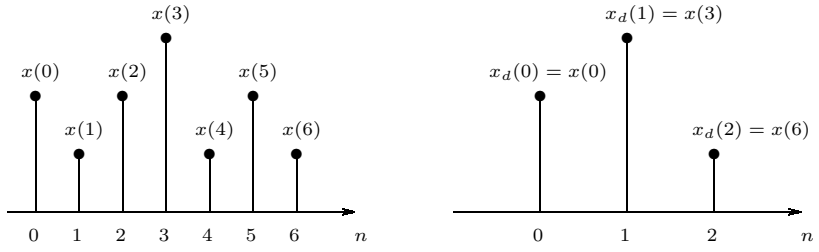

(a) A DT signal. (b) The result of downsampling.

Figure 1.67. Downsampling a signal by a factor of 3.

Let us now pretend that $x(n)$ was obtained by sampling a CT signal $x_c(t)$. Then $x(n) = x_c(nT_s)$, and, as shown above,

$$X(e^{j\omega}) = \frac{1}{T_s} \sum_n X_c \left(\frac{\omega - 2\pi n}{2\pi T_s} \right).$$

Moreover $x_d(n) = x_c(nDT_s)$, and so we can use the above formula with T_s replaced by DT_s to get:

$$X_d(e^{j\omega}) = \frac{1}{DT_s} \sum_n X_c \left(\frac{\omega - 2\pi n}{2\pi DT_s} \right). \tag{1.42}$$

To relate $X_d(e^{j\omega})$ to $X(e^{j\omega})$, we perform a change of variables:

$$n = k + rD, \text{ with } -\infty < r < \infty, \, 0 \le k \le D-1$$

Then we have

$$\begin{aligned} X_d(e^{j\omega}) &= \frac{1}{D} \sum_{k=0}^{D-1} \left[\frac{1}{T_s} \sum_{r=-\infty}^{\infty} X_c \left(\frac{(\omega - 2\pi k) - 2\pi rD}{2\pi DT_s} \right) \right] \\ &= \frac{1}{D} \sum_{k=0}^{D-1} \left[\frac{1}{T_s} \sum_{r=-\infty}^{\infty} X_c \left(\frac{\frac{\omega - 2\pi k}{D} - 2\pi r}{2\pi T_s} \right) \right] \\ &= \frac{1}{D} \sum_{k=0}^{D-1} X \left(e^{j\frac{\omega - 2\pi k}{D}} \right). \end{aligned} \tag{1.43}$$

The spectrum of the downsampled signal is therefore the sum of shifted replicas of the stretched spectrum of the original DT signal, as illustrated in Fig. 1.68.

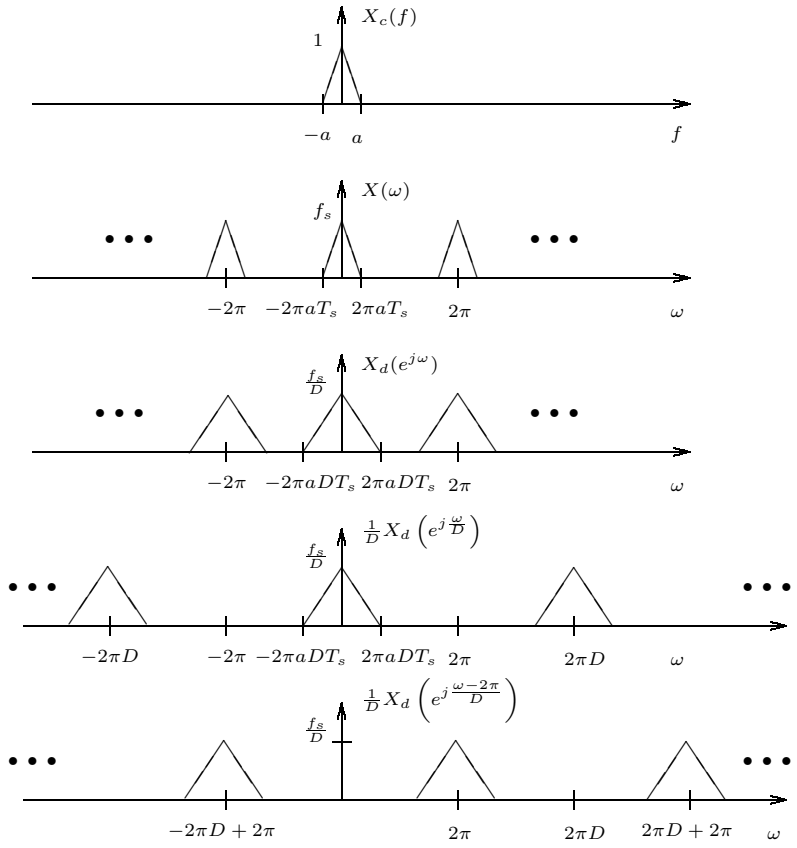

Figure 1.68. Comparison between signal spectra. In this pictorial example, $D = 2$. Refer to the derivation of Eq. (1.43).

From Fig. 1.68, when $2\pi aT_s D > \pi$, we have $2\pi aT_s > \frac{\pi}{D}$. This causes aliasing in the resulting spectrum.

Just as in the continuous-time case, we prefilter to avoid aliasing (Fig. 1.69).

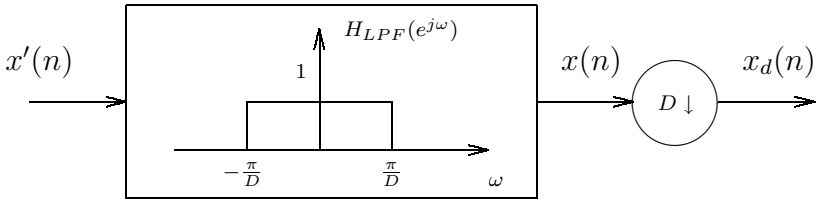

Figure 1.69. System diagram of a decimation scheme.